MAX-PLANCK-INSTITUT FÜR PLASMAPHYSIK

GARCHING BEI MÜNCHEN

Dispersion Curves for the Generalized Bernstein Modes

S. Puri, M. Tutter

IPP IV/42 August 1972

Die nachstehende Arbeit wurde im Rahmen des Vertrages zwischen dem Max-Planck-Institut für Plasmaphysik und der Europäischen Atomgemeinschaft über die Zusammenarbeit auf dem Gebiete der Plasmaphysik durchgeführt.

IV/42 S. Puri
M. Tutter

Dispersion Curves for the Generalized Bernstein Modes

August 1972 (in English)

A B S T R A C T

Dispersion curves are plotted for the extraordinary branch of the electron and ion cyclotron harmonic waves propagating perpendicularly to the static magnetic field in a non-relativistic, hot Maxwellian plasma, without invoking the electrostatic approximation. It is found that, except in the vicinity of the cyclotron harmonics and the hybrid resonances, either the cold-plasma or the electrostatic approximation are accurate representations of the exact solution. The hybrid resonances of the cold-plasma model become monotonically shrinking regions of low group velocity as the temperature is increased, till all discernible evidence of these resonances disappears as the parameters corresponding to the thermonuclear plasmas are approached.

1. INTRODUCTION

In this paper, numerically computed dispersion curves are presented for the electron and ion-cyclotron harmonic waves propagating perpendicularly to the static magnetic field in a hot Maxwellian plasma. Since the electrostatic approximation is not used and only the extraordinary waves are considered, the resultant modes are referred to as the generalized Bernstein modes, in the manner of Fredricks (1968). Instead of the usual Stepanov (Stix 1962) form of the hot plasma dielectric tensor, an equivalent derivation (possessing, however, greater elegance and symmetry) due to Derfler and Omura (1967) is employed in the computations.

Following the work of Gross (1951), Sen (1952), Gordeyev (1952), and Bernstein (1958), Dnestrovskij and Kostomarov (1961) undertook a detailed study of the hot Maxwellian plasma dispersion relation, both for the ordinary and the extraordinary electron modes, without invoking either the electrostatic approximation or the small parameter expansion used by the previous authors. They give accurately computed dispersion curves obtained from the complete hot-plasma dielectric tensor for a wide range of parameters, as well as their comparison with the cold-plasma and electrostatic approximations. Extensive computations of the electrostatic electron-cyclotron-harmonic waves with several different velocity distributions, as well as a bibliography of related work, are given by Crawford (1965) and Tataronis (1967). Work of Canobbio and Croci (1966) and Dougherty and Monaghan (1966) contain a thorough qualitative examination of the generalized electron Bernstein modes.

Outstanding among the studies of ion waves is the paper of Fredricks (1968) which, as we shall see later, is an uncannily accurate qualitative description of the generalized ion-Bernstein modes.

In addition to comparing our results with the references quoted above, the region of applicability of the electrostatic and the cold-plasma approximations, as well as the electric field polarizations, will be discussed. The relativistic effects are excluded at the outset, and a collisionless plasma model with a Maxwellian velocity distribution of equal electron and ion temperatures is assumed. Unless otherwise specified, the units used are relationalized MKS. The presentation of the electron and ion dispersion curves in § 4 and § 5, respectively, is preceded by brief descriptions of the cold-plasma dispersion in § 2 and of the Derfler-Omura hot plasma dielectric tensor in § 3.

2. C O L D - P L A S M A D I S P E R S I O N

The dispersion relation for the extraordinary wave in a cold, uniform plasma is given by (Stix 1962),

$$\frac{k_\perp^2 c^2}{\omega^2} \simeq \frac{(\omega^2 - \omega_{c1}^2)(\omega^2 - \omega_{c2}^2)}{(\omega^2 - \omega_{\ell h}^2)(\omega^2 - \omega_{uh}^2)} , \qquad (1)$$

where the equation

$$\omega^2 \mp \omega\omega_{ce} - \omega_{ce}\omega_{ci} - \omega_{pe}^2 = 0 \qquad (2)$$

is satisfied with the upper sign for $\omega = \omega_{c1}$ and with the lower sign for $\omega = \omega_{c2}$, and where $\omega_{\ell h}$ is the lower hybrid resonant frequency

$$\frac{1}{\omega_{\ell h}^2} = \frac{1}{\omega_{ci}^2 + \omega_{pi}^2} + \frac{1}{\omega_{ci}\,\omega_{ce}} \quad , \tag{3}$$

and ω_{uh} is the upper hybrid frequency

$$\omega_{uh}^2 = \omega_{pe}^2 + \omega_{ce}^2 \quad . \tag{4}$$

The two resonances $\omega_{\ell h}$ and ω_{uh} together with the two cut-off frequencies ω_{c1} and ω_{c2} combine to give a dispersion curve with three distinct branches (Fig.1) which will be referred to as the lower, the middle and the upper branch, respectively.

The hybrid resonances act as regions of strong wave absorption (Budden 1955) and have long been contenders for the heating of thermonuclear plasmas. One of the objectives of this work is the careful examination of the hot-plasma dispersion in the vicinity of these resonances.

3. H O T - P L A S M A D I S P E R S I O N

Instead of the Stepanov hot-plasma dielectric tensor (Stix 1962) in which the entire particle current is treated as the polarization current, we shall use the alternate description of Derfler and Omura (Omura 1967) in which the first order current density is subdivided into polarization and magnetization currents, so that the Maxwell's equations become

$$\nabla \times \vec{E} = - \frac{\partial}{\partial t} \left(\mu_o \overleftrightarrow{\mu} \vec{H} \right) \tag{5}$$

$$\nabla \times \vec{H} = \frac{\partial}{\partial t} \left(\epsilon_o \overleftrightarrow{\epsilon} \vec{E} \right) \tag{6}$$

$$\nabla \cdot \overleftrightarrow{\epsilon} \cdot \vec{E} = 0 \tag{7}$$

$$\nabla \cdot \overleftrightarrow{\mu} \cdot \vec{H} = 0 \tag{8}$$

where the dielectric and diamagnetic tensors $\overleftrightarrow{\epsilon}$ and $\overleftrightarrow{\mu}$, respectively, are given as

$$\overleftrightarrow{\epsilon} = \begin{bmatrix} \epsilon_{xx} & \epsilon_{xy} & 0 \\ \epsilon_{yx} & \epsilon_{yy} & 0 \\ 0 & 0 & \epsilon_{zz} \end{bmatrix} \tag{9}$$

and

$$\overleftrightarrow{\mu} = \begin{bmatrix} \mu_{xx} & \mu_{xy} & 0 \\ \mu_{yx} & \mu_{yy} & 0 \\ 0 & 0 & \mu_{zz} \end{bmatrix} \tag{10}$$

For an isotropic Maxwellian particle velocity districation the dielectric tensor components are given by

$$\epsilon_{xx} = \epsilon_{yy} = 1 + \sum_j \frac{\omega_p^2 \epsilon_o}{2 \omega \omega_c} \exp(-\lambda) \sum_{-\infty}^{\infty} I_n(\lambda) \left(Z_{n+1} - Z_{n-1} \right) , \tag{11}$$

$$\epsilon_{zz} = 1 - \sum_j \frac{\omega_p^2}{\omega^2} \varsigma_0^2 \exp(-\lambda) \sum_{-\infty}^{\infty} I_n(\lambda) Z_n' , \tag{12}$$

$$\epsilon_{xy} = -\epsilon_{yx} = \sum_j s_j \frac{i \omega_p^2 \varsigma_0}{\omega \omega_c} \exp(-\lambda) \sum_{-\infty}^{\infty} I_n(\lambda) \left(Z_n - \frac{Z_{n+1} + Z_{n-1}}{2} \right) , \tag{13}$$

where,

$$\varsigma_n = \frac{\omega - n\omega_c}{k_{\parallel}} \left(\frac{1}{2\eta\theta} \right)^{1/2} , \tag{14}$$

$$\lambda = \frac{\eta \theta k_{\perp}^2}{\omega_c^2} = k_{\perp}^2 r_c^2 \tag{15}$$

j denotes the particle type, $s_j = \pm 1$ is the sign of the charge carried by the particle, η is its charge to mass ratio, θ is the temperature expressed in volts, r_c is the cyclotron radius, $I_n(\lambda)$ is the modified Bessel function in the notation of Watson (1922) and $Z_n = Z(\varsigma_n)$ is the Fried function (Fried and Conte 1961) defined as

$$Z(\varsigma_n) = \pi^{-1/2} \int_{-\infty}^{\infty} \frac{e^{-x^2}}{x - \varsigma_n} dx , \quad Im[\varsigma_n] > 0 . \tag{16}$$

Relations similar to (11 - 13) exist for the $\overleftrightarrow{\mu}$ tensor also.

We stress that, apart from appearance, the Stepanov and the Derfler-Omura tensors are entirely equivalent (Omura 1967). This has been independently confirmed by Leuterer and Tutter (1972). In fact, O'Sullivan (1972) has derived the Derfler-Omura

tensor from the relativistic tensor of Trubnikov (1959) using appropriate limits. Although, in the context of the present undertaking, no significant computational advantage accrues by using either one of the two forms of the dielectric tensors, we prefer the Derfler-Omura description which, unlike the Stepanov tensor, satisfies the Onsager relations even when both k_x and k_y are non-zero (see Cato et al. 1971).

For the parameter ranges used in this paper, we have confirmed through direct computations that

$$\left| \mu_{\alpha\beta} - I_{\alpha\beta} \right| < 10^{-3} \tag{17}$$

provided that

$$\Delta\omega = |\omega - n\omega_c| > 10^{-2}\,\omega_c \,, \tag{18}$$

where $\overleftrightarrow{I}$ is the identity tensor. If we confine our attention to the frequency region defined by (18), we may replace $\overleftrightarrow{\mu}$ by $\overleftrightarrow{I}$. With this provision, the dispersion relation for perpendicular propagation can be factored into ordinary and extraordinary waves in the standard manner. For the extraordinary mode,

$$(k_\perp / k_o)^2 = (\epsilon_{xx}^2 + \epsilon_{xy}^2) / \epsilon_{xx} \,. \tag{19}$$

In the subsequent sections, dispersion curves obtained by the numerical solution of (19) are presented.

4. THE ELECTRON MODES

For perpendicular propagation $\xi_n \to \infty$, $Z_n \to -1/\xi_n$, so that (11) and (13) become

$$\epsilon_{xx} = 1 - 2 \sum_j \frac{\omega_p^2}{\omega^2} \frac{\exp(-\lambda)}{\lambda} \sum_1^\infty \frac{n^2 I_n(\lambda)}{\omega^2 - n^2 \omega_c^2} \qquad (20)$$

$$\epsilon_{xy} = -i \sum_j s_j \frac{\omega_p^2}{\omega\, \omega_{ce}} \exp(-\lambda) \left[\frac{\omega_c^2}{\omega^2 - \omega_c^2} I_0(\lambda) \right.$$

$$\left. - \sum_1^\infty I_n(\lambda) \left\{ \frac{2\omega^2}{\omega^2 - (n+1)^2 \omega_c^2} - \frac{2\omega^2}{\omega^2 - n^2 \omega_c^2} + \frac{\omega^2}{\omega^2 - (n-1)^2 \omega_c^2} \right\} \right] \qquad (21)$$

For the electron modes further simplication occurs by neglecting the small icn contribution because $\omega_{pi}^2/\omega^2 << 1$ so that (20) and (21) yield,

$$\epsilon_{xx} = 1 - 2\pi_e^2 \frac{\exp(-\lambda_e)}{\lambda_e} \sum_1^\infty \frac{n^2 I_n(\lambda_e)}{1 - n^2 \Omega_e^2} \qquad (22)$$

$$\epsilon_{xy} = \frac{i \pi_e^2}{\Omega_e} \exp(-\lambda_e) \left[\frac{\Omega_e^2}{1 - \Omega_e^2} I_0(\lambda_e) \right.$$

$$\left. + \sum_1^\infty I_n(\lambda_e) \left\{ \frac{1}{1 - (n+1)^2 \Omega_e^2} - \frac{2}{1 - n^2 \Omega_e^2} + \frac{1}{1 - (n-1)^2 \Omega_e^2} \right\} \right] \qquad (23)$$

where $\pi_e = \omega_{pe}/\omega$ and $\Omega_e = \omega_{ce}/\omega$. The infinite summations of (22) and (23) are truncated for some N such that the inequalities

$$I_n(\lambda) / I_0(\lambda) < 10^{-5} \qquad (24)$$

and

$$\left| \exp(-\lambda) \left\{ I_0(\lambda) + 2 \sum_{1}^{N} I_n(\lambda) \right\} - 1 \right| < 10^{-5} \qquad (25)$$

are satisfied. The second of these inequalities (Abramowitz and Stengun 1964, § 9.6.38) constitutes an independent check on the accuracy of In(λ). The two inequalities together ascertain that the tensor components of $\overleftrightarrow{\epsilon}$ are computed with an accuracy exceeding one part in a thousand in the frequency region defined by (18). Substituting the values of ϵ_{xx} and ϵ_{xy} obtained from (22) and (23), the dispersion relation (19) can be solved using standard iteration techniques. In general, an infinite set of solutions exists for the transcendental dispersion relation. However, we shall confine our attention to the solutions with real ω and k values.

The dispersion curves so obtained for two different values of r_{ce}^2 are shown in Figs.2 and 3. At low values of r_{ce}^2, the upper-hybrid resonance of the cold plasma is replaced by a "plateau" of low group velocity (Fig.2) which in turn vanishes for higher values of r_{ce}^2 (Fig.3). A somewhat different qualitative behaviour at the hybrid frequency occurs (Fig.4) for the case $\omega_{ce} < \omega_{uh} < 2\omega_{ce}$ when no real solutions exist in the region $\omega_{uh} < \omega < 2\omega_{ce}$ so that the "plateau" near ω_{uh} extends over a much wider range of k. Apart from contributing these observations in the vicinity of the upper-hybrid frequency, our results are essentially similar to the dispersion curves of Dnestrovskij and Kostamorov (1961). We shall not dwell on other cases involving different values of ω_{uh}, ω_{c1} and ω_{c2}

because the structure of the dispersion curves is predictable and resembles that of Figs.2 and 3.

A comparison of the generalized Bernstein modes with the electrostatic and cold-plasma approximations is shown in Figs. 5 and 6 for the parameters of Figs.2 and 3, respectively. (In these and some later plots, parts of the dispersion curves have been omitted to facilitate clearer presentation.) It is seen that these two approximations yield between them accurate information about the exact solution except near the upper-hybrid frequency, where the exact solution lies somewhere between the two approximations. For the set of modes lying just underneath $n\omega_{ce}$, however, there is no counterpart in either the cold plasma or the electrostatic approximations.

The generalized Bernstein modes are elliptically polarized being electrostatic (k || E) for large k. This is clearly seen from Fig.7 where dashed lines (dotted in regions of uncertain computational accuracy) represent contours of constant value of the ratio R given by

$$R = \left| E_x / E_y \right|$$

where E_x and E_y are the electric field components along the directions k and k x B, respectively. R typically exceeds 1oo in the region of validity of the electrostatic approximation. At the two cutoffs ω_{c1} and ω_{c2}, R = 1 corresponding to circular polarization (Pfirsch and Tutter 1963).

5. THE ION MODES

For the ion modes $\lambda_e \ll 1$, and (2o) and (21) simplify to

$$\epsilon_{xx} = 1 + \frac{\pi e^2}{\Omega e^2} - 2\pi_i^2 \frac{\exp(-\lambda_i)}{\lambda_i} \sum_1^\infty \frac{n^2 I_n(\lambda_i)}{1 - n^2 \Omega_i^2} \qquad (27)$$

$$\epsilon_{xy} = -i \frac{\pi i^2}{\Omega_i} \exp(-\lambda_i) \left[\frac{\Omega_i^2}{1 - \Omega_i^2} I_o(\lambda_i) \right.$$

$$\left. + \sum_1^\infty I_n(\lambda_i) \left\{ \frac{1}{1 - (n+1)^2 \Omega_i^2} - \frac{2}{1 - n^2 \Omega_i^2} + \frac{1}{1 - (n-1)^2 \Omega_i^2} \right\} \right] \qquad (28)$$

The exact solution, as well as the cold-plasma and electrostatic approximations for two different values of r_{ci}^2, are shown in Figs.8 and 9. As in the case of the upper-hybrid resonance, the cold-plasma resonance at the lower-hybrid frequency is replaced by a plateau of low group velocity (Fig.8) which gradually disappears as the temperature is raised (Fig.9). Similar conclusions regarding the behaviour at the lower-hybrid frequency have been just reported by Nambu (1972) during the preperation of this manuscript. For the case $\omega_{ci} < \omega_{\ell h} < 2\omega_{ci}$ no real solutions exist for $\omega_{\ell h} < \omega < 2\omega_{ci}$ as in the case of the electron modes. These results are in exact agreement with the qualitative curves of Fredricks (1968). Finally, the polarization of the ion modes characterized by the ratio R defined in (26) is shown in Fig.1o. All ion mode computations have been performed using the Deuterium mass.

6. DISCUSSION AND CONCLUSIONS

The electron and ion modes of Fig.3 and 9, respectively, drawn for parameters resembling thermonuclear conditions show that the hybrid resonances can not be expected to play a direct role in the rf heating of thermonuclear plasmas.

Unlike the electron modes, the ion modes possess a fast electromagnetic branch below the hybrid frequency. This fast wave has a cutoff ($k \to o$ as $\omega \to n\omega_{ci}$ from above) and a region of low group velocity ($\partial\omega/\partial k \to o$ as $\omega \to n\omega_{ci}$ from below). The inclusion of damping either due to collisions or finite $k_{\parallel}$ could lead to ion heating (Wharton 1971) if the waves launched in a high magnetic field region approached a "beach" where $\omega \to n\omega_{ci}$. Similar effects may cause the slow wave to damp in either a decreasing or an increasing magnetic field as $\omega \to n\omega_{ci}$ from either below or above. It may then be possible that in thermonuclear plasmas, the cyclotron-harmonic absorption mechanism will be an effective replacement for the heating at the hybrid resonances.

ACKNOWLEDGEMENTS

We express our sincere gratitude to Frau Stöckermann for carrying out the extensive computations reported here.

R E F E R E N C E S

ABRAMOVITZ M., STEGUN I.A., 1964, Handbook of Mathematical Functions, Washington D.C., National Bureau of Standards

BERNSTEIN I.B., 1958, Phys. Rev. 1o9, 1o

BUDDEN K.G., 1955, Proc. Roy. Soc. A227, 516

CANOBBIO E., CROCI R., 1966, Phys. Fluids 9, 549

CATO J.E., KRISTIANSEN M., MAGLER M.O., 1971, Wave Propagation and Damping in a Hot, Bounded Plasma, Report No. ORO-3778-6, Texas Tech. Univ., Lubbock, Texas, p.8

CRAWFORD F.W., 1965, Nucl. Fusion 5, 73

DNESTROVESKIJ Yu.N., KOSTOMAROV D.P., 1961, JETP 4o, 14o4; 1961, Soviet Phys. JETP 13, 986

DNESTROVESKIJ Yu.N., KOSTOMAROV D.P., 1961, JETP 41, 1527; 1962, Soviet Phys. JETP 14, 1o89

DOUGHERTY J.P., MONAGHAN S.S., 1966, Proc. Roy. Soc. A289, 214

FREDRICKS R.W., 1968, J. Plasma Phys. 2, 365

GORDEYEV G.V., 1952, JETP 6, 66o

GROSS E.P., 1951, Phys. Rev. 82, 232

LEUTERER F., TUTTER M., 1972, private communication

NAMBU M., 1972, J. Plasma Phys. 7, 5o3

OMURA M., 1967, Electrostatic Waves in Bounded Hot Plasmas, SUIPR Report No. 156, Stanford University, Stanford, Calif.

O'SULLIVAN R., 1972, private communication

PFIRSCH D., TUTTER M., 1963, Anregung und Nachweis von Plasmawellen durch Feldwellen, Report MPI-PA-15/63, Max-Planck-Institut für Physik und Astrophysik, Munich

SEN H.K., 1952, Phys. Rev. 88, 816

STIX T.H., 1962, Theory of Plasma Waves, New York, McGraw Hill Book Co.

TATARONIS J.A., 1967, Cyclotron Harmonic Waves Propagation and Instabilities, SUIPR Report No. 2o5, Stanford University, Stanford, Calif.

TRUBNIKOV B.A., 1958, Plasma Physics and the Problem of Controlled Thermonuclear Reactions, 3, 1o4

WATSON G.N., 1922, Theory of Bessel Functions, Cambridge University Press

WHARTON C.B., KORN P., ROBERTSON S., 1971, Phys. Rev. Lett. 27, 499

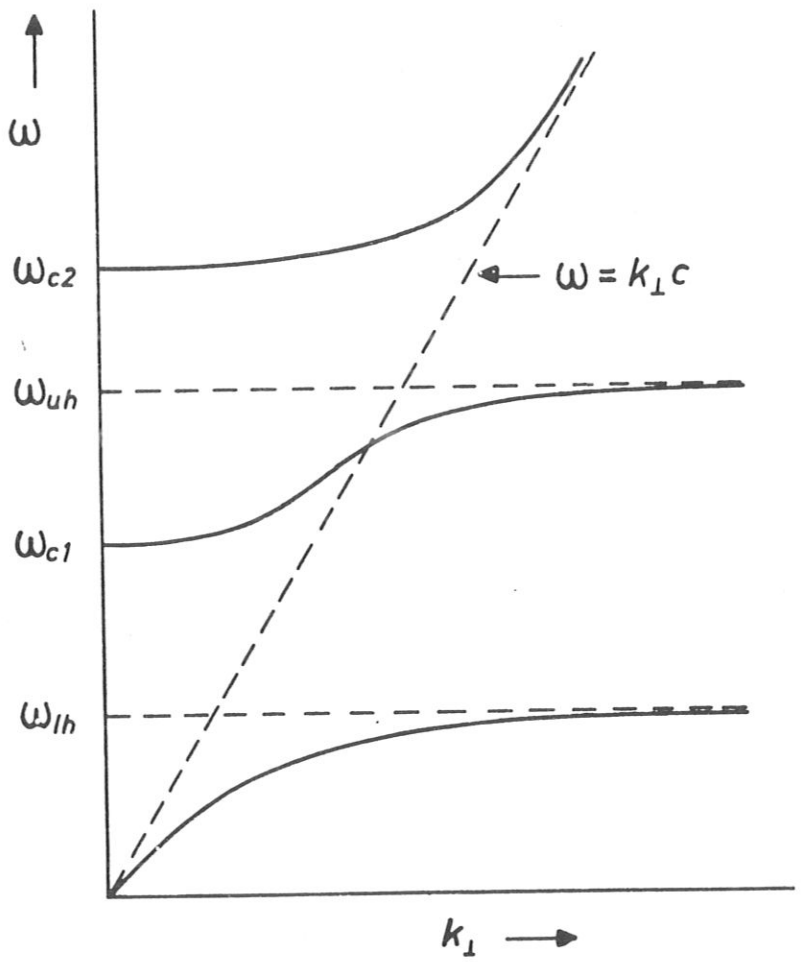

Fig. 1 The cold plasma dispersion

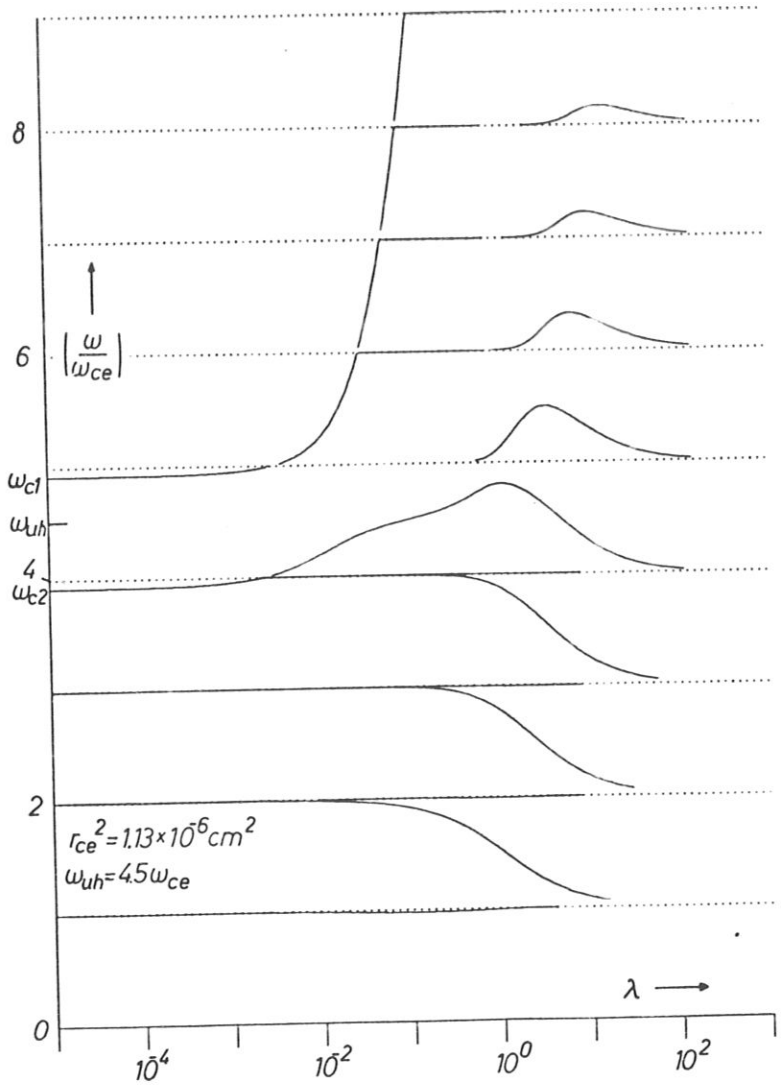

Fig. 2 Generalized electron Bernstein modes with $r_{ce}^2 = 1.13 \times 10^{-6}$ cm^2 and $\omega_{uh} = 4.5\ \omega_{ce}$

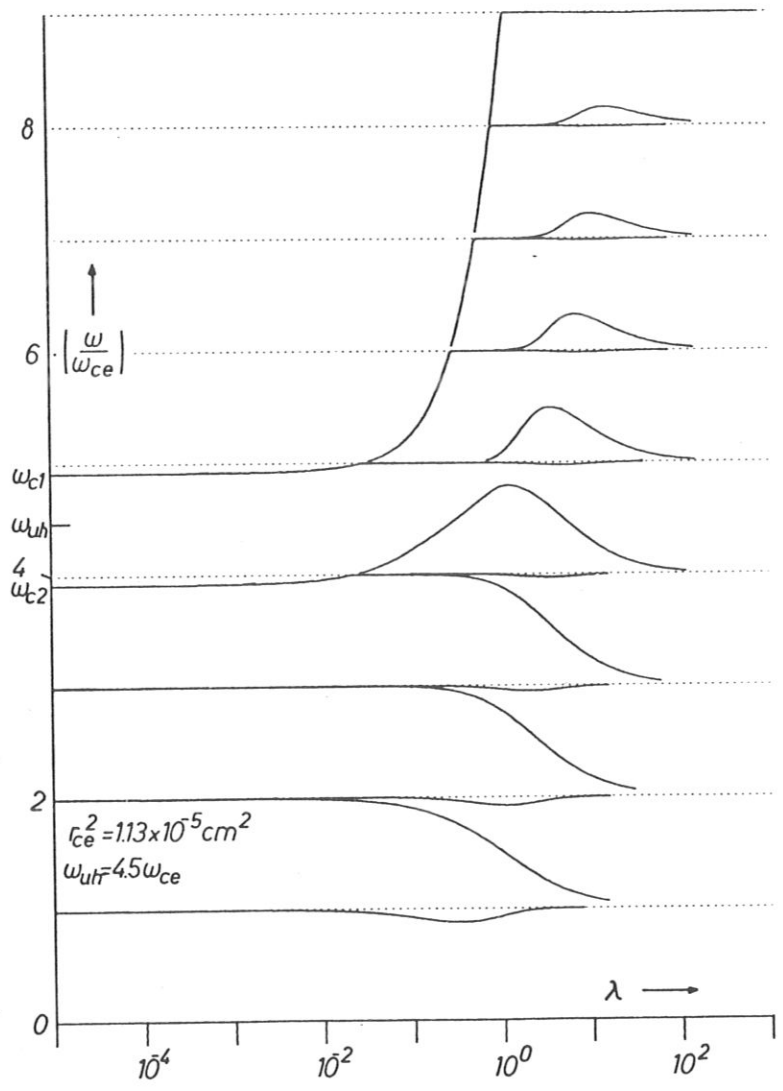

Fig. 3 Generalized electron Bernstein modes with $r_{ce}^2 = 1.13 \times 10^{-5}$ cm^2 and $\omega_{uh} = 4.5\ \omega_{ce}$

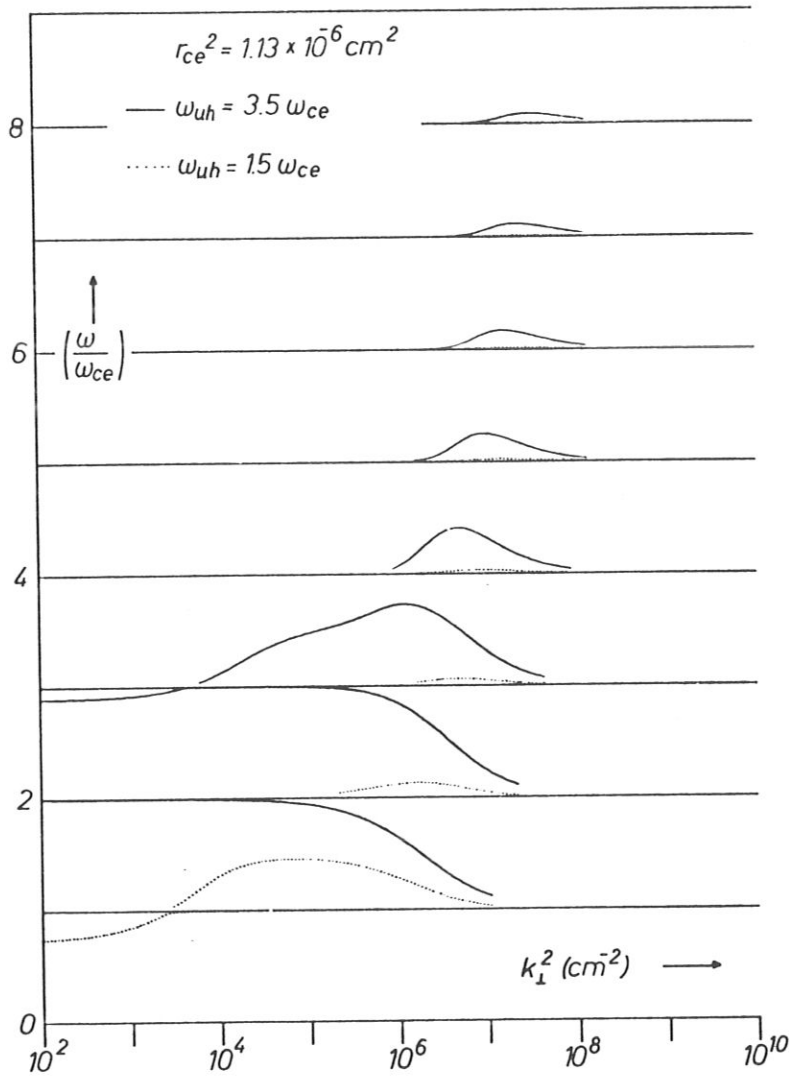

Fig. 4 Generalized electron Bernstein modes with $r_{ce}^2 = 1.13 \times 10^{-6}$ cm^2, and $\omega_{uh} = 3.5\ \omega_{ce}$ (solid curve) and $\omega_{uh} = 1.5\ \omega_{ce}$ (dotted curve)

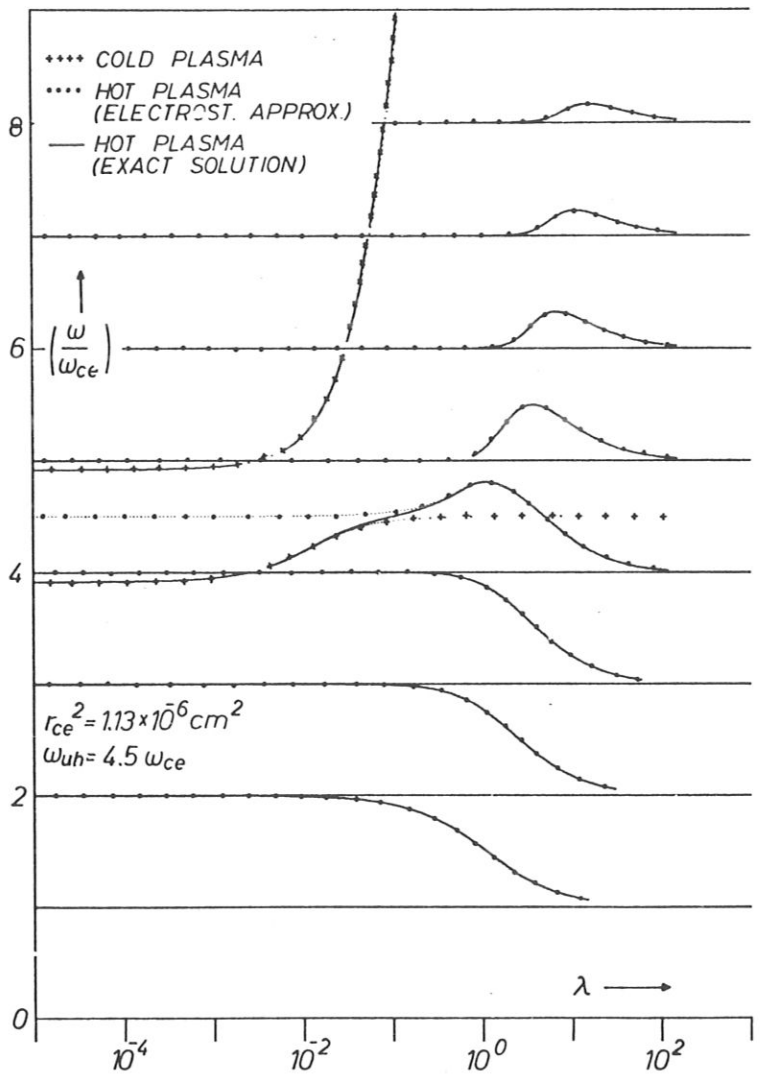

Fig. 5 Comparison of the exact solution of the electron modes with the electrostatic and cold-plasma approximations with $r_{ce}^2 = 1.13 \times 10^{-6}$ and $\omega_{uh} = 4.5\ \omega_{ce}$

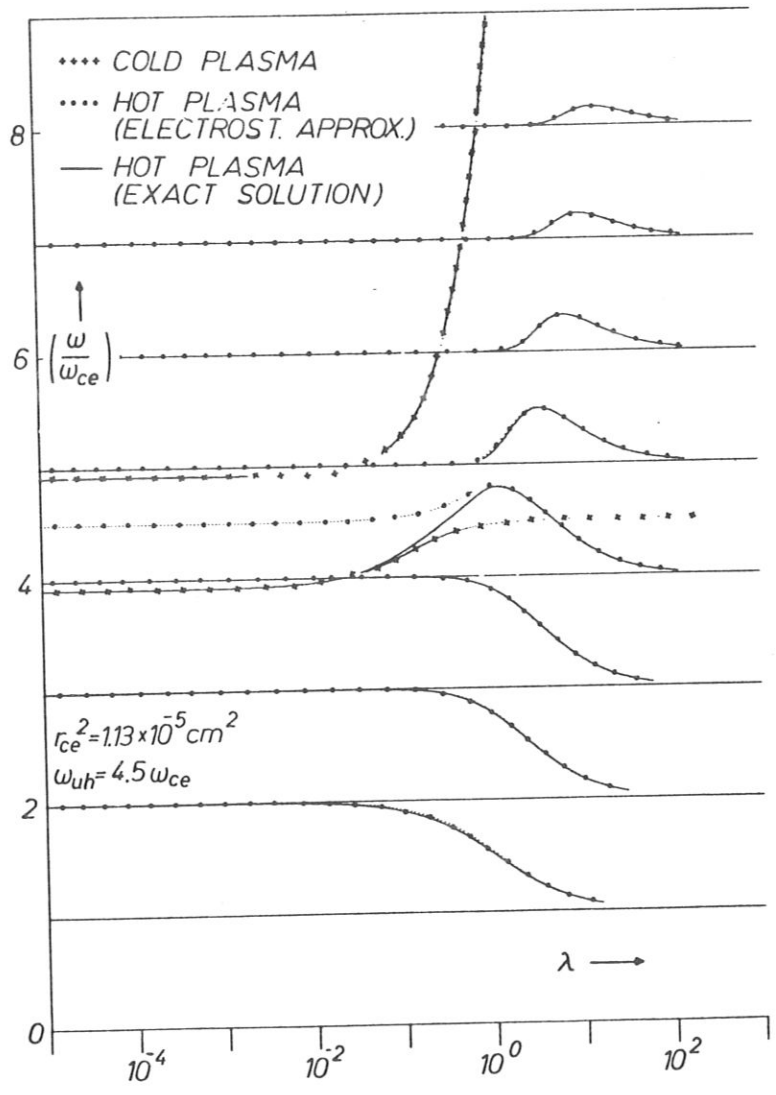

Fig. 6 Comparison of the exact solution of the electron modes with the electrostatic and cold-plasma approximations with $r_{ce}^2 = 1.13 \times 10^{-5}\ cm^2$ and $\omega_{uh} = 4.5\ \omega_{ce}$

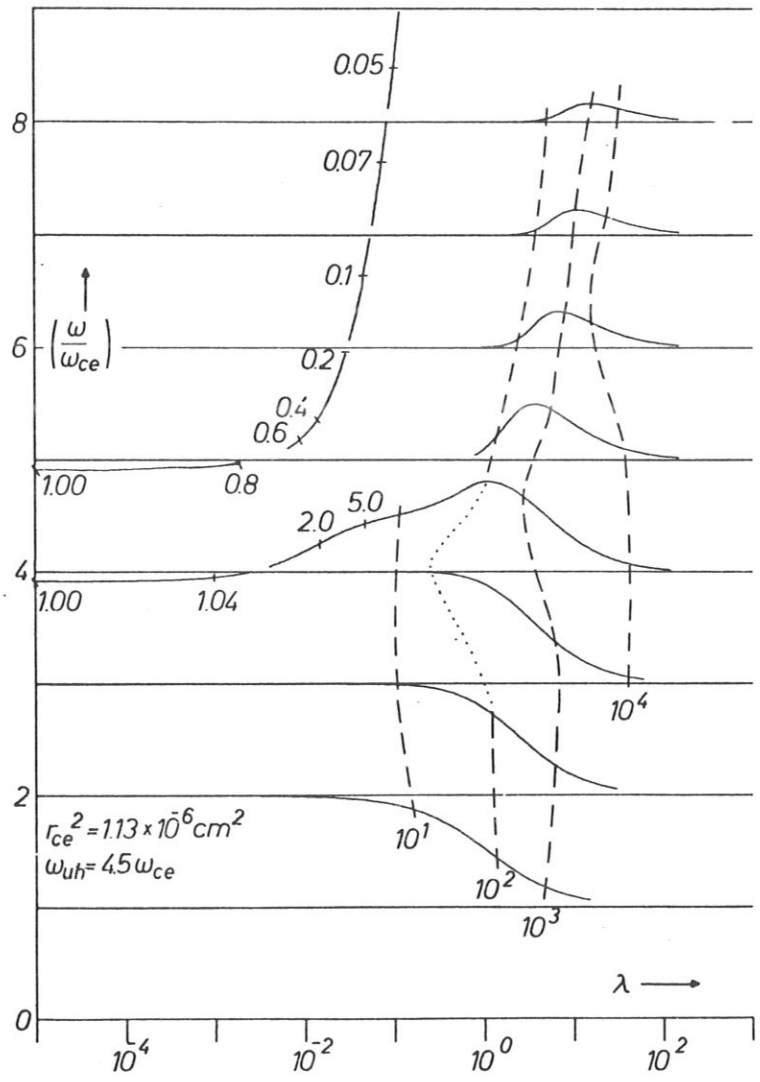

Fig. 7 The polarization of the generalized electron Bernstein modes. The dashed lines (dotted in regions of uncertain computational accuracy) are contours of constant R defined in (26)

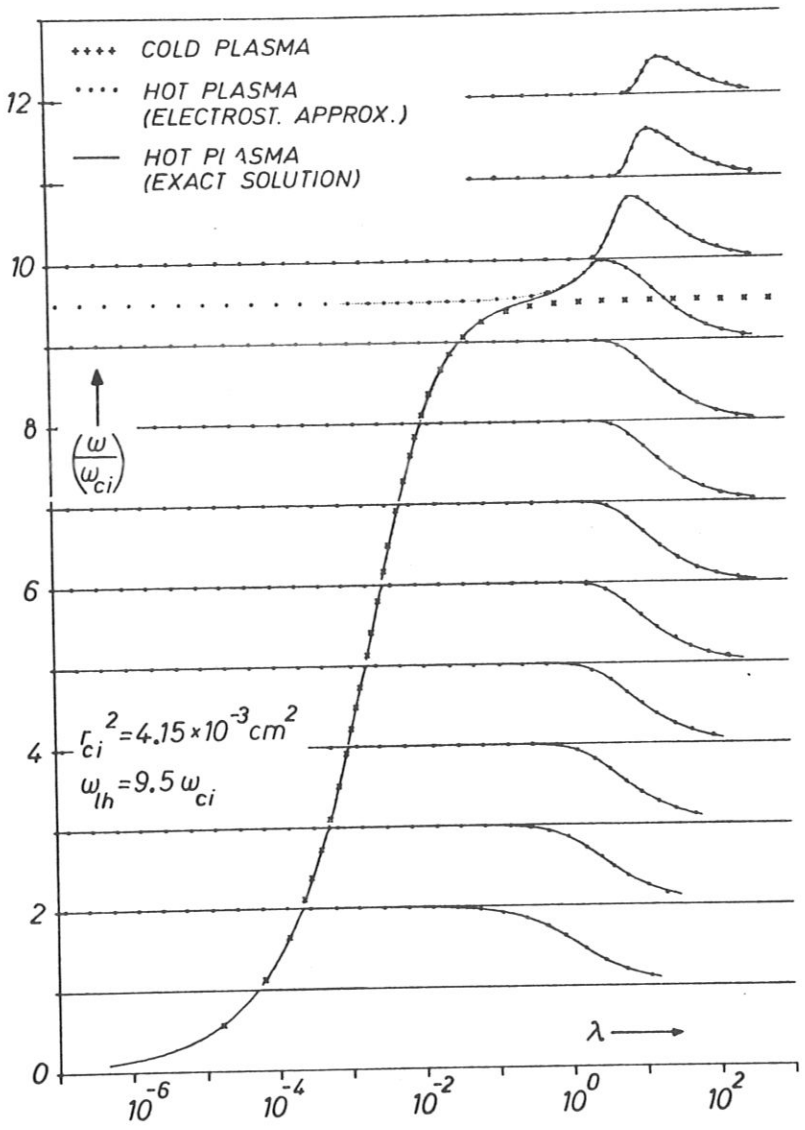

Fig. 8 Comparison of the exact solution of the ion modes with the electrostatic and cold-plasma approximations with $r_{ci}^2 = 4.15 \times 10^{-3}$ cm^2 and $\omega_{lh} = 9.5\, \omega_{ci}$

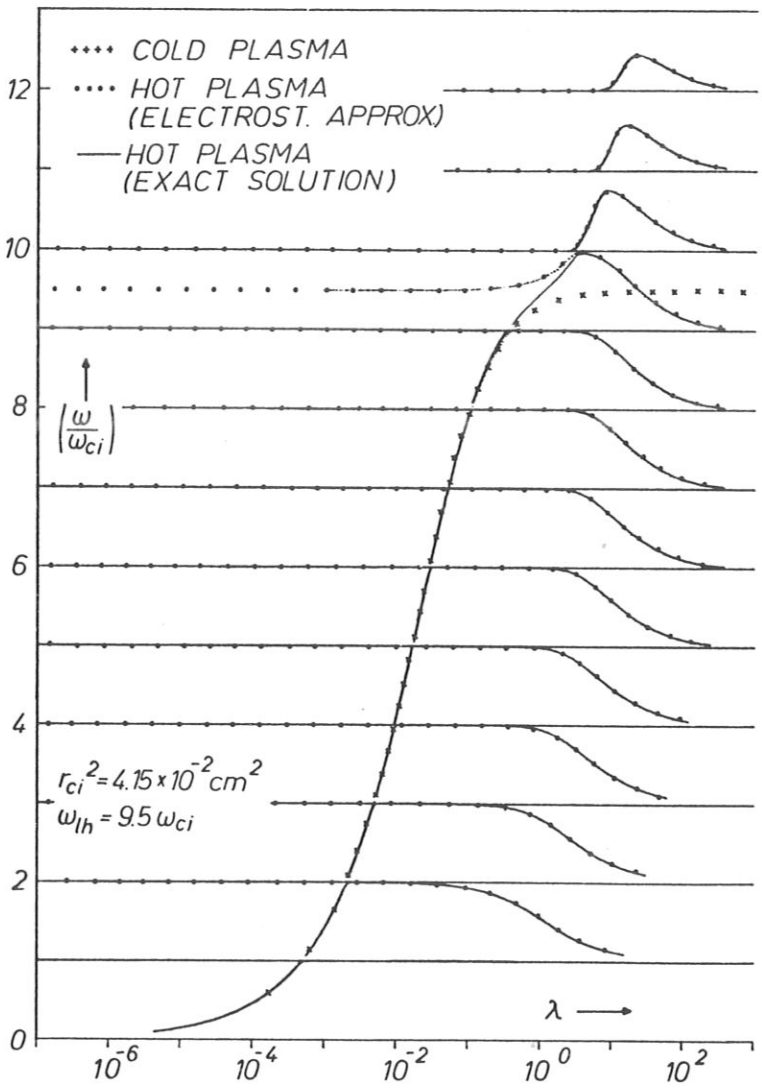

Fig. 9 Comparison of the exact solution of the ion modes with the electrostatic and cold-plasma approximations with $r_{ci}^2 = 4.15 \times 10^{-2}\ cm^2$ and $\omega_{\ell h} = 9.5\ \omega_{ci}$

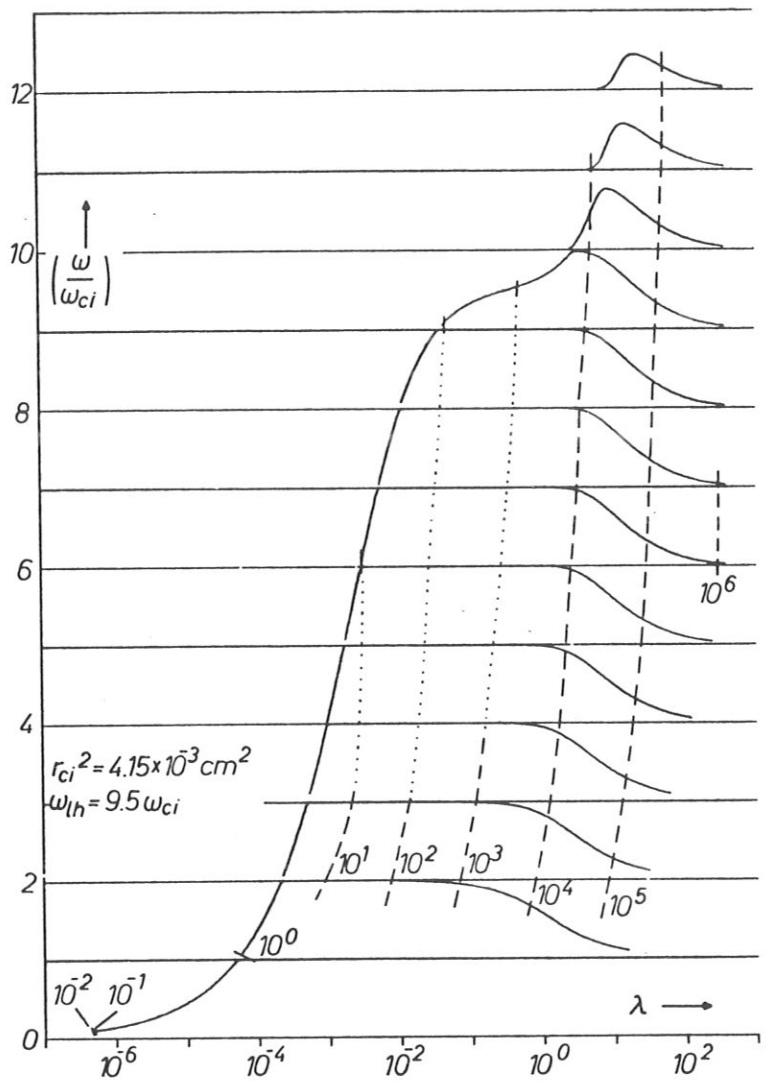

Fig. 1o The polarization of the generalized ion Bernstein modes. The dashed lines (dotted in regions of uncertain computational accuracy) are contours of constant R defined in (26)